Available online at www.sciencedirect.com
SCIENCE DIRECT®
Journal of Electroanalytical Chemistry 568 (2004) 93–99
Journal of Electroanalytical Chemistry
www.elsevier.com/locate/jelechem

Voltammetric studies on nitro radical anion formation from furazolidone and kinetic of the coupled chemical reaction

Lida Fotouhi *, Sara Faramarzi

Department of Chemistry, Faculty of Science, Al-Zahara University, P.O. Box 1993891176, Tehran, Iran

Received in revised form 11 December 2003; accepted 17 January 2004
Available online 6 May 2004

Abstract

The electrochemical behavior of the nitro radical anion, $RNO_2^{\cdot-}$, of furazolidone has been investigated to study the tendency of $RNO_2^{\cdot-}$ to undergo further chemical reaction. The study was carried out in dimethylformamide (DMF) + water mixtures at different pH values on both mercury (Hg) and glassy carbon (GC) electrodes. The subsequent chemical reaction corresponds to a second order process; protonation of the electrogenerated $RNO_2^{\cdot-}$. The procedure of Olmstead et al. [Anal. Chem. 41 (1969) 260] was employed to calculate the second order rate constant, k_2. The k_2 values are strongly pH-dependent. The interaction of $RNO_2^{\cdot-}$ with cysteine has been studied on a GC electrode, and the apparent rate constant, k_{app}, reported.

Keywords: Coupled chemical reaction; Cyclic voltammetry; Kinetic; Furazolidone; Chronoamperometry

1. Introduction

Electrochemical reactions of aromatic nitro compounds have been studied extensively [1]. In acidic media all nitro compounds are reduced in two cathodic processes giving hydroxylamine and amine derivatives via reduction by four and two electrons, respectively. It has been reported that nitro compounds can generate a reversible 1-electron process due to formation of the nitro radical anion ($RNO_2^{\cdot-}$) and an irreversible 3-electron process corresponding to formation of the hydroxylamine (RNHOH) in aprotic media [2–4].

The main pharmaceutical uses of nitro aromatic compounds are as antibacterial and anticancer agents [5–7]. The reduction of these compounds is believed to be due to flavoproteins known as "nitro reductases" which have the ability to use nitro compounds as acceptors of one or two electrons [8]. Thus, in the case of the 1-electron metabolic reduction pathway, the nitro radical anion results. This species exhibits cytotoxicity in several cellular systems [9–12], by reacting with oxygen at a faster rate than the ability of the enzyme to add a second electron. One reason for our interest in studying the kinetics of the nitro radical anion of furazolidone as a drug is that this species, as a free radical, has great significance in biological metabolisms. Furazolidone is a drug with a nitro group in its structure (Fig. 1), it is a highly effective chemotherapeutic drug, and widely used to control common infections in humans and animals.

Electrochemistry, specifically cyclic voltammetry, plays an important role in the study of free radicals [13]. There are several papers [14–16] related to the 1-electron reduction of nitro aromatic compounds in order to form $RNO_2^{\cdot-}$, which can be protonated and further reduced.

Zuman et al. [17,18] have indicated the dependence of the potential and current of the cathodic peaks of nitrobenzene on pH and reported their protonation constants. They also have shown how the peak potentials depend on the structure of the nitro compound and DMF concentration. Several studies have been reported on the polarographic determination of furazolidone [19,20] in the literature, but little attention has been paid to the formation and kinetics of the coupled chemical reaction of nitro radical anion generated electrochemically from furazolidone. There are some reports on the kinetic parameters of some drugs [21–24].

* Corresponding author. Tel.: +98-21-8044051; fax: +98-21-8047861.
E-mail address: lfotouhi@alzahra.ac.ir (L. Fotouhi).

0022-0728/$ - see front matter © 2004 Elsevier B.V. All rights reserved.
doi:10.1016/j.jelechem.2004.01.009

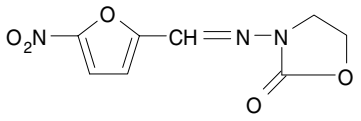

Fig. 1. Molecular structure of furazolidone.

In previous work [25] we have found that $RNO_2^{\cdot-}$ resulting from furazolidone can be stabilized at aprotic media and the effect of the addition of surfactants on this stability was demonstrated. In continuation of our interest in the electrochemistry of biologically active organic [26–28] compounds, we thought it is worthwhile to review our work on the kinetics of $RNO_2^{\cdot-}$ generated electrochemically from furazolidone in mixed media of dimethylformamide + water (40:60 and 60:40) on both glassy carbon and mercury electrodes.

2. Experimental

2.1. Reagents and solutions

Furazolidone was purchased from Sigma for basic studies. All the other reagents employed were of analytical grade without further purification. 1 mM furazolidone solution was used in mixed dimethylformamide + aqueous solution (60:40 and 40:60) media. The aqueous solutions were 0.015 M sodium citrate and 0.05 M boric acid. The pH was adjusted with small aliquots of concentrated NaOH or HCl, respectively. The ionic strength was kept constant with aqueous 0.30 M KCl. Dimethylformamide (DMF) and tetrabutylammonium perchlorate (TBAP) were used in aprotic media as solvent and supporting electrolyte, respectively.

2.2. Apparatus

Cyclic voltammetric experiments were carried out with a Metrohm model 746 VA trace analyzer connected a 747 VA stand. A glassy carbon electrode (0.2 mm diameter) was used as the working electrode which was polished sequentially with alumina powder and after rinsing with doubly distilled water, was repeatedly scanned in the range 1400 to −1400 mV in 0.1 M $NaHCO_3$. A multimode mercury electrode (Metrohm) was also used as a working electrode. A platinum wire and a commercial KCl saturated Ag|AgCl electrode from Metrohm were used as the auxiliary and reference electrodes, respectively.

2.3. Methods

The experimental I_a/I_c ratios were calculated according to the procedure of Nicholson and Shain [29], using individual cyclic voltammograms. A further switching potential (E_λ) was selected in order to minimize the influence of the second cathodic peak.

The second order rate constant, k_2, was obtained from the cyclic voltammetry method according to Olmstead et al. [30]. Second order coupled reactions occupy a significant role in cyclic voltammetry. In a second order irreversible coupled chemical reaction following an electron transfer reaction (EC_i) the I_a/I_c ratio decreased with increasing concentration [30]. The positive portion of the cyclic voltammogram is most sensitive to the rate of the coupled chemical reaction. Thus, the I_a/I_c values measured experimentally at each scan rate were inserted into the working curve to determine ω [30] which incorporates the effects of rate constant, concentration and scan rate.

For each of the switching potentials (E_λ) the I_a/I_c ratios were plotted against the quantity $\log\omega$ (working curve). ω is defined from the following equation [30]:

$$\omega = k_2 c_0 \tau, \tag{1}$$

where k_2 is the second order rate constant for decomposition of $RNO_2^{\cdot-}$, c_0 is the nitro compound concentration and τ is the time from $E_{1/2}$ to E_λ ($\tau = (E_\lambda - E_{1/2})/\upsilon$), υ is the scan rate.

The assumption that the decomposition of $RNO_2^{\cdot-}$ follows second order kinetics is supported by the linear relation between ω (which was calculated graphically from experimental ratios of I_a/I_c) and τ.

Several authors [31,32] have studied the interaction of the nitro radical anion with some thiol compounds; prompted by these reports, we chose to study the interaction of furazolidone with cysteine. To assess the reactivity of $RNO_2^{\cdot-}$ with cysteine, the effect of cysteine concentration on the nitro radical anion at different scan rates was studied.

In the case of any interaction between $RNO_2^{\cdot-}$ and cysteine the I_a/I_c ratio must be decreased by increasing cysteine concentration. Thus $RNO_2^{\cdot-}$ has two possible modes for decay in the presence of cysteine as follows:

$$2RNO_2^{\cdot-} + 2H^+ \xrightarrow{k_2} RNO_2 + RNO + H_2O$$

$$RNO_2^{\cdot-} + RSH \xrightarrow{k_i} \text{Product}$$

To estimate quantitatively the interaction rate constant (k_i) for the reaction between $RNO_2^{\cdot-}$ and cysteine, the following considerations were taken into account. The overall rate of decay of the $RNO_2^{\cdot-}$ species can be expressed as [22]

$$\frac{-\mathrm{d}[RNO_2^{\cdot-}]}{\mathrm{d}t} = 2k_2[RNO_2^{\cdot-}]^2 + k_i[\text{cysteine}][RNO_2^{\cdot-}]. \tag{2}$$

An apparent second order rate constant, k_{app}, can be defined as

$$k_{app} = 2k_2 + k_i[\text{cysteine}]/[RNO_2^{\cdot-}]. \tag{3}$$

In the absence of cysteine, $k_{app} = 2k_2$. As can be seen, k_2 is a pH-dependent rate constant and it is valid for a buffered medium, and could be considered an apparent second order constant. Thus, if Eq. (3) is divided by $2k_2$, the following final expression is obtained:

$$\frac{k_{app}}{2k_2} = 1 + k_i[\text{cysteine}]/2k_2[\text{RNO}_2^{\cdot-}]. \quad (4)$$

If $[\text{RNO}_2^{\cdot-}]$ is kept constant, the plot of $k_{app}/2k_2$ vs. cysteine concentration should be linear with a slope of $k_i/2k_2[\text{RNO}_2^{\cdot-}]$. Since k_2 is known and $[\text{RNO}_2^{\cdot-}]$ is assumed equal to the nitro compound concentration it is possible to obtain the rate constant for the interaction between cysteine and furazolidone.

Double-potential-step chronoamperometry has proven useful for investigating the EC mechanism [33]. The signal was a square-wave voltage signal with initial potential, $E_i = -0.65$ V, step potential, $E_s = -0.35$ V, final potential, $E_f = -0.65$ V and interval of time, $\tau = 5$ s. If there is no coupled chemical reaction, the forward current, I_f (cathodic current), is equal to the backward current, I_b (anodic current). On the other hand, if the ratio I_b/I_f decreases with increasing time, there is a chemical reaction following electron transfer (EC mechanism). Chronoamperometry has been used for the measurement of the diffusion coefficient, D, of the electroactive species. D can then be calculated from the average value of $jt^{1/2}$ over a range of time via the Cottrell equation [33]:

$$j = \frac{I}{A} = \frac{nFD^{1/2}c_0}{\pi^{1/2}t^{1/2}} = kt^{-1/2}, \quad (5)$$

where D is the diffusion coefficient ($cm^2\ s^{-1}$), c_0 is concentration (M), t is time (s) and j is current density (mA cm^{-2}).

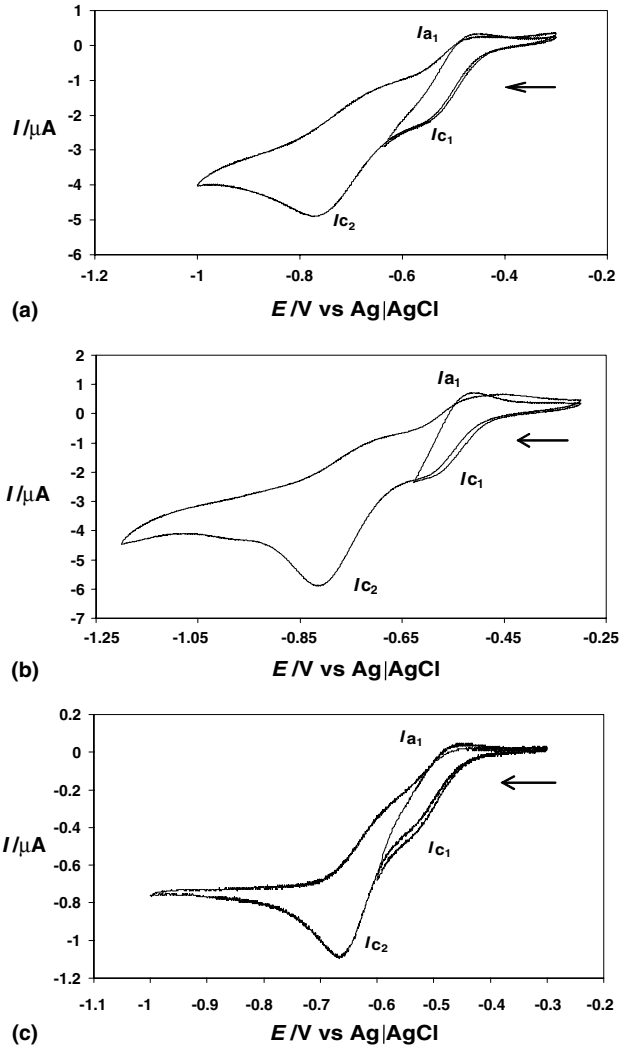

Fig. 2. The cyclic voltammograms of furazolidone (a) at 40% DMF on a GC electrode, (b) at 60% DMF on a GC electrode, (c) at 40% DMF on the Hg electrode, pH 8.8, scan rate 20 mV s^{-1}.

3. Results and discussion

The cyclic voltammogram of furazolidone in protic media shows two reductive peaks due to the 4-electron and 2-electron reduction of the nitro group to form the corresponding hydroxylamine (RNHOH) and amine (RNH_2), respectively, as is usual for nitroaromatic compounds [19–22,25] (data not shown). The reduction mechanism is different on changing from a protic to an aprotic medium. In other word, by adding the DMF (or at high pH) (Fig. 2) the peak due to a 4-electron transfer was changed to a 1e-reversible peak corresponding to $\text{RNO}_2^{\cdot-}$ (Ic_1 and Ia_1) with a subsequent more negative 3e-irreversible peak due to RNHOH (Ic_2 without any reverse peak) according to the following equations:

$$\text{RNO}_2 + e^- \rightleftharpoons \text{RNO}_2^{\cdot-}$$

$$\text{RNO}_2^{\cdot-} + 3e^- + 4H^+ \rightarrow \text{RNHOH} + H_2O$$

However, in this work our current interest is devoted to the study of the $\text{RNO}_2^{\cdot-}$ in mixed media (40–60% DMF + aqueous media) with both mercury and glassy carbon electrodes as working electrodes to find the reduction mechanism of $\text{RNO}_2^{\cdot-}$ and its kinetic coupled chemical reaction.

In Fig. 2, the cyclic voltammograms of furazolidone in mixed media containing 40% (Fig. 2(a)) and 60% DMF (Fig. 2(b)) at pH 8.8 on a GC electrode are shown. As can be seen, the 1e-reversible peak is due to the RNO_2/ $\text{RNO}_2^{\cdot-}$ couple (Ec_1) and 3e-irreversible reductive peak (Ec_2) corresponding to the formation of RNHOH. The same voltammetric behavior of furazolidone also appeared on the mercury electrode (Fig. 2(c)). The potential values for 40% and 60% of DMF at both electrodes are shown in Table 1.

From the results in Table 1, it can be concluded that the DMF percentage showed a greater influence at Ec_2,

Table 1
The potential values of the $RNO_2/RNO_2^{\cdot-}$ couple of furazolidone at a scan rate of 20 mV s^{-1} and an apparent pH value of 8.8

%DMF	GC electrode			Hg electrode		
	$-E_1$ (V)	$-E_2$ (V)	ΔE_c[a] (V)	$-E_1$ (V)	$-E_2$ (V)	ΔE_c[a] (V)
40	0.57	0.75	0.18	0.56	0.66	0.10
60	0.59	0.81	0.22	0.58	0.76	0.18

[a] $\Delta E_c = |Ec_1 - Ec_2|$.

than Ec_1, so Ec_2 shifted to more negative potentials with increasing DMF percentages. Thus, the potential separation was increased by increasing DMF percentage (from 0.18 to 0.22 V at GC and from 0.10 to 0.18 V at the Hg electrode). From the above experiments we can appreciate that, for the same % DMF solution, the use of GC as the working electrode produces a shift of the 3e-irreversible peak to more negative potentials. Consequently, the ΔE_c was increased on GC when compared with the Hg electrode. By considering that the 3e-step involves a first protonation of $RNO_2^{\cdot-}$ with further reduction, the shift of potentials to more negative potential can be attributed to hindrance of the protonation.

When different electrodes were used, it seems that the adsorption of the nitro radical anion is stronger at mercury than at a GC electrode [34].

The cyclic voltammograms of furazolidone at different concentrations are shown in Fig. 3. The linear plot of current vs. concentration shows a diffusion-controlled process (Fig. 3, inset, top). The I_a/I_c ratio decreased with increasing concentration (Fig. 3, inset, bottom). On the other hand, the slope of the plot of E_p vs. $\log c$ is 23 mV which is in good agreement with the theoretical value of 19 mV for an EC_i process where the chemical reaction follows second order kinetics [35–37].

In order to study the kinetics of $RNO_2^{\cdot-}$ we have studied in isolation the couple due to the first electron transfer. It is clear that the negative potential of furazolidone is pH-independent, while the I_a/I_c ratio increased toward unity with increasing pH in both 40% and 60% DMF at both electrodes (Table 2).

Table 2
The I_a/I_c ratios for two DMF percentages and at two electrodes for 1 mM furazolidone and a scan rate of 100 mV s^{-1}

pH	I_a/I_c on GC		I_a/I_c on Hg	
	40% DMF	60% DMF	40% DMF	60% DMF
8.00	0.818	0.765	0.786	0.796
8.45	0.850	0.809	0.818	0.868
8.80	0.880	0.850	0.826	0.900
9.42	0.920	0.934	0.900	0.947
10.00	0.978	1.000	0.956	1.000

From the above results the most probable mechanism was suggested as follows:

$$RNO_2 + e^- \rightleftharpoons RNO_2^{\cdot-}$$

$$2RNO_2^{\cdot-} + 2H^+ \xrightarrow{k_2} RNO_2 + RNO + H_2O$$

Typical cyclic voltammograms of furazolidone at different scan rates at pH 9.0 are shown in Fig. 4. As can be seen from Fig. 4 the I_a/I_c ratio increased toward unity with increasing scan rate. This diagnostic citation fulfils the requirements for an irreversible chemical reaction following a reversible electron transfer (EC_i process). In order to study this mechanism, the effects of both pH and scan rate were studied. In the typical graphs of Fig. 5, we show the results obtained by varying both scan rate and pH at 40% DMF on a GC electrode. Similar experiments were obtained for the two DMF percentages on both electrodes. In all cases the I_a/I_c

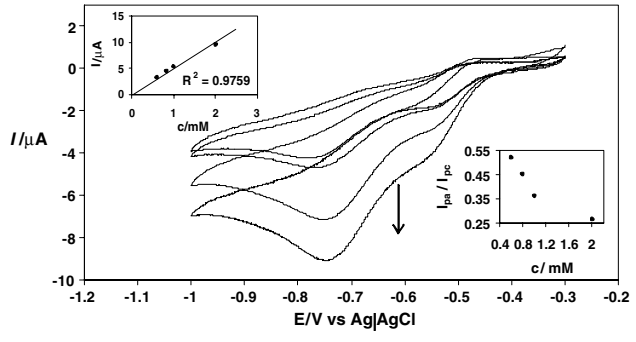

Fig. 3. The cyclic voltammograms of furazolidone at different concentration, 0.6, 0.8, 1.0 and 2.0 mM, on a GC electrode, pH 8.8, 40% DMF. Inset (top): the plot of current vs. concentration, inset (bottom): the plot of I_a/I_c vs. concentration.

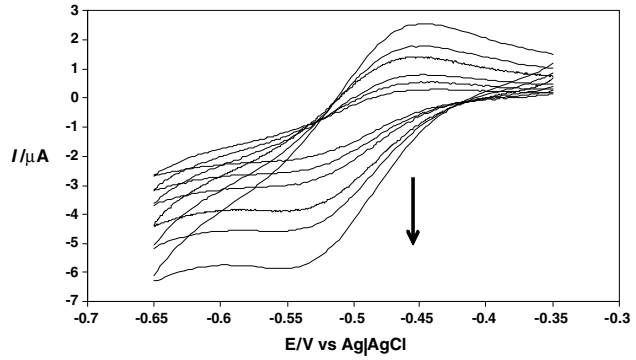

Fig. 4. The cyclic voltammograms of furazolidone at different scan rates: 25, 40, 60, 100, 150 and 250 mV s^{-1}, pH 9.0, 40% DMF, on a GC electrode.

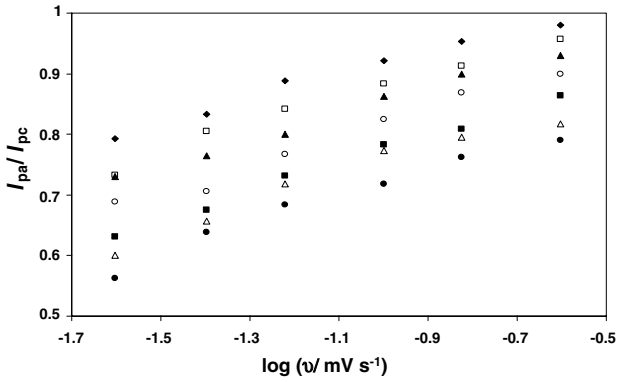

Fig. 5. The plot of I_a/I_c vs. $\log \upsilon$ at different pH, 40% DMF, on a GC electrode, (◆) pH 10.20, (□) pH 9.97, (▲) pH 9.62, (○) pH 9.29, (■) pH 9.0, (△) pH 8.78, (●) pH 8.50.

increased toward one with increase of both the pH and scan rate.

In order to obtain the second order rate constants, k_2, the I_a/I_c values measured experimentally at each scan rate were inserted into the working curve to determine ω. Figs. 6(a) and (b) show the plots of ω vs. τ for both DMF percentages on the GC electrode. From the slopes of these lines k_2 values were obtained for the decay of $RNO_2^{\cdot-}$ at different pH values, which are strongly pH-dependent. The dependences of k_2 with pH are shown in Fig. 7(a) at the GC electrode. In all cases, the stability of $RNO_2^{\cdot-}$ was increased by the increasing pH and DMF percentage. Similar behavior was also obtained for furazolidone at the Hg electrode (Fig. 7(b)).

Double potential step chronoamperometry has proven useful for investigating the EC_i mechanism. As can be seen from the chronoamperogram of furazolidone in Fig. 8, the ratio of forward current (I_f) to backward current (I_b) decreased with increasing time, which confirms an EC_i process. It can be seen from Fig. 8 (inset) that the $jt^{1/2}$ values are constant at prolonged time, thus the averaged value of $jt^{1/2}$ is equal to $nFD^{1/2}c_0/\pi^{1/2}$. As all constant parameters are known, a value of the

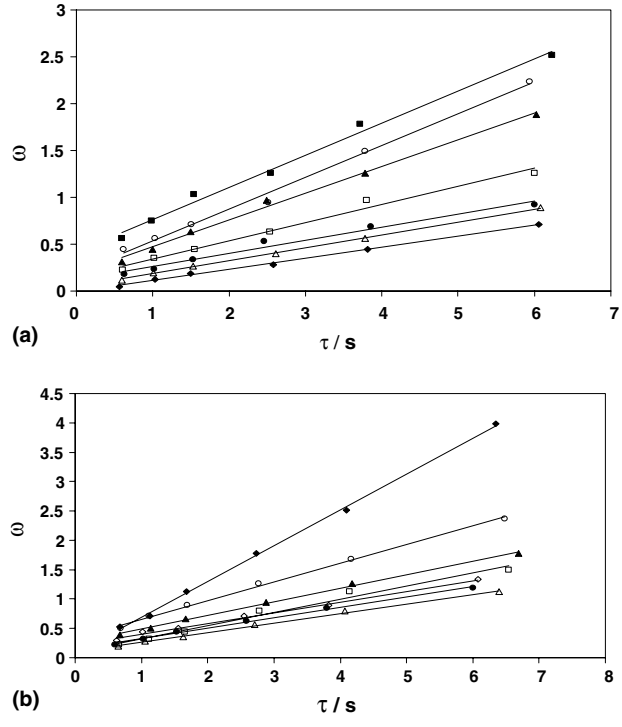

Fig. 6. The plot of ω vs. τ on a GC electrode (a) 40% DMF, (◆) pH 10.20, (△) pH 9.97, (●) pH 9.62, (□) pH 9.29, (▲) pH 9.00, (○) pH 8.78, (■) pH 8.50, (b) 60% DMF, (△) pH 9.82, (●) pH 9.68, (◇) pH 9.28, (□) pH 9.05, (▲) pH 8.68, (○) pH 8.41, (◆) pH 8.22.

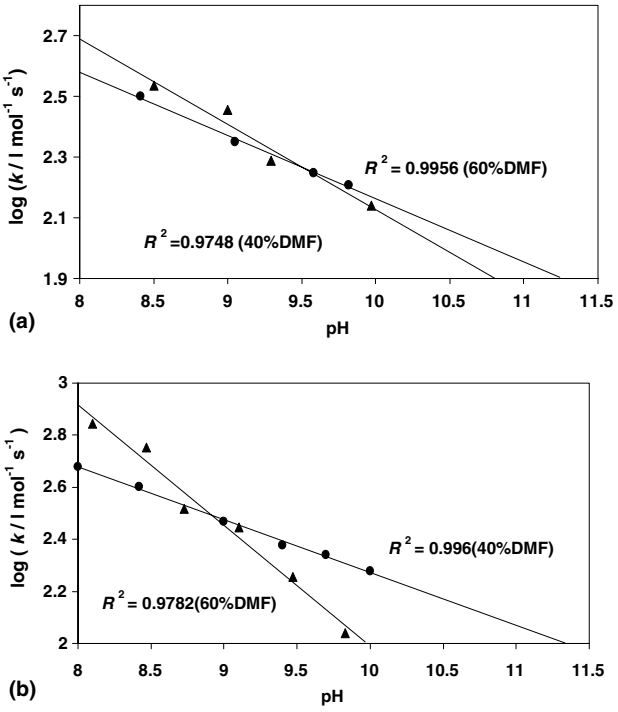

Fig. 7. The plot of $\log k$ vs. pH at 40% and 60% DMF (a) on the GC electrode (b) on the Hg electrode.

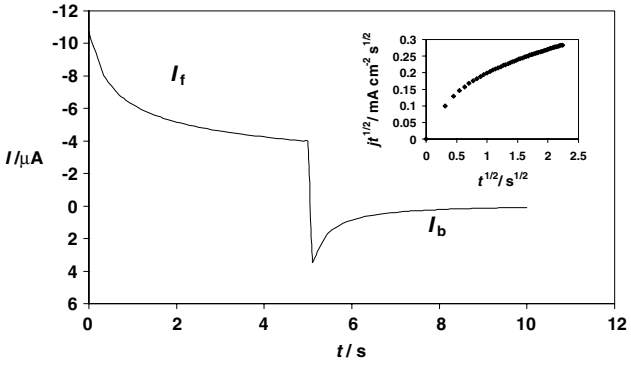

Fig. 8. The chronoamperogram of furazolidone on a GC electrode. 40% DMF, pH 8.8, $E_i = -0.65$ V, $E_s = -0.35$ V, $E_f = -0.65$ V, and $\tau = 5$ s. Inset: The plot of $jt^{1/2}$ vs. $t^{1/2}$.

diffusion coefficient of 2.64×10^{-5} cm^2 s^{-1} was obtained for furazolidone.

The studies concerning the interaction of the $RNO_2^{\cdot-}$ with thiol compounds show that thiol compounds react significantly with the nitro radical anion [22,38–40]. Several workers have postulated that the cytotoxicity of nitroaromatic compounds arises from the reaction of $RNO_2^{\cdot-}$ with RSH [9–11]. To assess the potential cytotoxicity of nitro radical anion generated from furazolidone, the interaction of furazolidone with cysteine was investigated on a GC electrode. The cyclic voltammograms of furazolidone in the presence of different concentrations of cysteine are shown in Fig. 9. A decrease of the I_a/I_c ratio with increasing cysteine concentration (Fig. 9, inset) is a good indication of the interaction of these compounds.

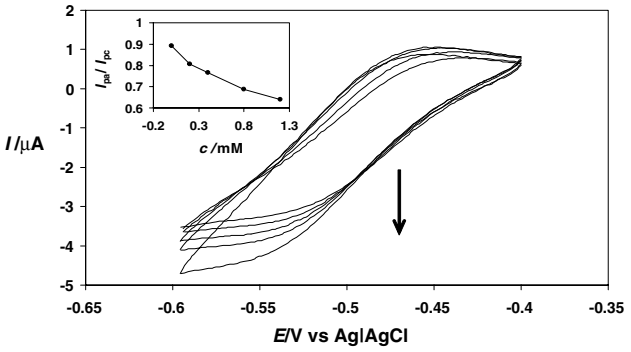

Fig. 9. The cyclic voltammograms of furazolidone in the presence of different cysteine concentrations: 0.20, 0.40, 0.80, 1.20 mM, 40% DMF, scan rate 100 mV s^{-1}, on the GC electrode. Inset: The plot of I_a/I_c vs. cysteine concentration.

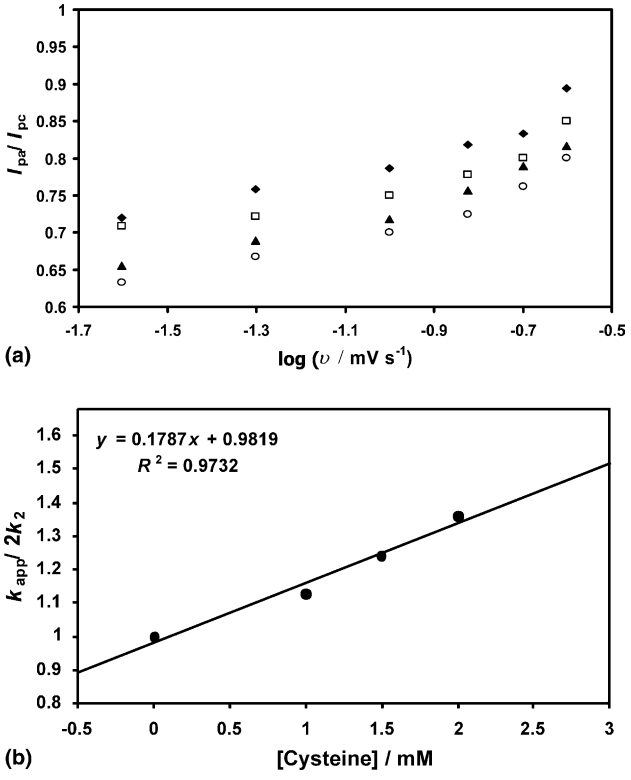

Fig. 10. (a) The plot of I_a/I_c vs. log υ at different cysteine concentrations, pH 8.5, 40% DMF, on the GC electrode, (◆) 0 mM, (□) 1 mM, (▲) 1.5 mM, (○) 2 mM (cysteine). (b) The plot of $k_{app}/2k_2$ vs. different cysteine concentrations, pH 8.5, on the GC electrode.

Fig. 10(a) shows a typical I_a/I_c vs. log υ plot at pH 8.5 and 40% DMF on the GC electrode. Fig. 10(b) shows the plot of $k_{app}/2k_2$ vs. cysteine concentration. k_i values of 0.40×10^2 and 0.52×10^2 l mol^{-1}s^{-1} were obtained at pH 8.5 and 9.0, respectively, on the GC electrode.

4. Conclusion

Furazolidone is a synthetic nitrofuran drug which is effective as an antibacterial agent. In this research we studied the cyclic voltammograms focused on the coupled chemical reaction of the electrogenerated nitro radical anion. From our results it is found that a protonation chemical reaction followed the electron transfer reduction of furazolidone. The chronoamperometry also showed an EC_i mechanism and the diffusion coefficient of furazolidone was obtained as 2.64×10^{-5} cm^{2}s^{-1}. The use of a higher percentage DMF solution (60%) caused an increase in the separation of the 1e-reversible and 3e-irreversible peaks.

The pH effect shows that the potential peaks remained unaltered, while the current ratio was changed. Thus, protons have an effect on the coupled chemical reaction. The protonation chemical reaction follows a second order reaction and the EC_i mechanism was confirmed by both cyclic voltammetry and chronoamperometry.

The pH-dependence of k_2 with a different electrode surface and DMF content is shown. In all experiments the stability of the nitro radical anion increased with increasing pH, i.e. when the proton concentration decreased, the decay reaction was not favored. On the other hand, at the higher DMF percentage solution the decay increased.

As the cytotoxicity of nitro compounds arises from the reaction of $RNO_2^{\cdot-}$ with thiol, the interaction of cysteine with the nitro radical anion was studied. On the other hand, most thiol compounds can react with mercury [41], thus the interaction of furazolidone with cysteine was investigated only on the GC electrode. The interaction rate constant of cysteine with $RNO_2^{\cdot-}$ from furazolidone was found to be 0.40×10^2 and 0.52×10^2 l mol^{-1} s^{-1} at pH values of 8.5 and 9.0, respectively, which is a good indication that cysteine behaves as a scavenger of the nitro radical anion generated from furazolidone, thus providing experimental proof of the ability of cysteine to trap this type of species. Furthermore, it can be concluded that furazolidone can poten-

tially behave as a cytotoxic drug, which produces the nitro radical anion and the oxygen tension present in the cells. The relevance of the latter factor lies in the fact that it permits the rapid reoxidation of the radical; thus, the risk of cytotoxity is minimized in aerobic mammalian cells. The toxicity of nitro drugs lies in their ability to exert a cytotoxic effect in anaerobes which can reduce the nitro group, and the resulting $RNO_2^{\cdot-}$ is responsible for their strand-breaking effects on DNA [9–12,22].

Acknowledgements

The authors express their gratitude for financial support from the Department of Chemistry of Al-Zahra University. Financial support from Dr. S. Haghgoo is also acknowledged.

References

[1] W. Kenmula, T.M. Krygowski, A.J. Bard, H. Lund (Eds.), Encyclopedia of Electrochemistry of the Elements, vol. 13, Marcel Dekker, New York, 1979, p. 77.
[2] M. Heyrovsky, S. Vavricka, L. Holleck, B. Kastening, J. Electroanal. Chem. 26 (1970) 399.
[3] A. Darchen, P. Boudeville, Bull. Soc. Chim. Fr. (1971) 3809.
[4] M. Heyrovsky, S. Vavricka, J. Electroanal. Chem. 43 (1973) 311.
[5] D. Greenwood, Antimicrobial Chemotherapy, 13th ed., Oxford University Press, Oxford, 1995.
[6] L.P.L. Logan, P.A. Gummet, J.J. Misiewicz, Q.N. Karim, M.M. Walker, G.H. Baron, Lancet II (1991) 1449.
[7] G.E. Adams, Radiat. Res. 132 (1992) 129.
[8] J.E. Biaglow, B. Jarabson, C.L. Greenstock, J. Kaleigh, Mol. Pharmacol. 13 (1977) 269.
[9] J.E. Biaglow, M.E. Varnes, L. Roizer-Towle, E.P. Clark, E.R. Epp, M.B. Astor, E.J. Hall, Biochem. Pharmacol. 35 (1986) 77.
[10] J.R. Ames, V. Hollstein, A.R. Gogneux, M.D. Ryan, P. Kovacevic, Free Rad. Biol. Med. 3 (1987) 85.
[11] J.R. Ames, M.D. Ryan, P. Kovacevic, Free Rad. Biol. Med. 2 (1986) 277.
[12] R.C. Knight, I.M. Skolimokski, D.I. Edwards, Biochem. Pharmacol. 27 (1978) 2089.
[13] L.H. Piette, P. Ludwing, R. Aams, Anal. Chem. 34 (1962) 916.
[14] I. Rubinstein, J. Electroanal. Chem. 183 (1985) 379.
[15] C.K. Mann, K.K. Barnes, A.J. Bard (Eds.), Electrochemical Reactions in Non-Aqueous Systems, Marcel Dekker, New York, 1970, p. 11.
[16] E. Brillas, G. Farnia, M. Severin, E. Vianello, J. Electrochim. Acta 31 (1986) 759.
[17] P. Zuman, Z. Fijalek, J. Electroanal. Chem. 296 (1990) 583.
[18] C. Karakus, P. Zuman, J. Electroanal. Chem. 396 (1995) 499.
[19] T. Galeano Diaz, A. Guiberteau Cabenillas, Anal. Chim. Acta 273 (1993) 351.
[20] A.G. Cabenillas, T.G. Diaz, A. Espinosa-Mansilla, P.L. Lopez-de-Alba, F. Salinaz Lopez, Anal. Chim. Acta 302 (1995) 9.
[21] L.J. Nunez-Vergara, S. Bollo, A. Alvarez, M. Blazquez, J.A. Squella, J. Electroanal. Chem. 345 (1993) 129.
[22] L.J. Nunez-Vergara, F. Garcia, M. Dominguez, J. De Ia Fuente, J.A. Squella, J. Electroanal. Chem. 381 (1995) 215.
[23] J.H. Tocher, D.L. Edwards, Free Rad. Res. Commun. 4 (1988) 269.
[24] J.H. Tocher, D.L. Edwards, Free Rad. Res. Commun. 16 (1992) 19.
[25] L. Fotouhi, L. Kiapasha, Polish J. Chem. (submitted).
[26] L. Fotouhi, N. Maleki, A. Safavi, J. Electroanal. Chem. 399 (1995) 229.
[27] A. Safavi, L. Fotouhi, J. Electroanal. Chem. 434 (1997) 93.
[28] L. Fotouhi, F. Hajilari, M.M. Heravi, Electroanalysis 14 (2002) 1728.
[29] R.S. Nicholson, I. Shain, Anal. Chem. 36 (1964) 1406.
[30] M.L. Olmstead, R.G. Hamilton, R.S. Nicholson, Anal. Chem. 41 (1969) 260.
[31] A. Radi, F. Belal, J. Electroanal. Chem. 441 (1998) 39.
[32] J.H. Tocher, D.I. Edwards, Biochem. Pharmacol. 48 (1994) 1089.
[33] A.J. Bard, L.R. Faulkner, Electrochemical Methods Fundamental and Applications, Wiley, New York, 1980.
[34] J.M. Lopez-Fanseco, M.C. Gomez Rivera, J.C. Garcia Monteaguda, E. Uriarit, J. Electroanal. Chem. 347 (1993) 277.
[35] B.K. Eggins, N.H. Smith, Anal. Chem. 51 (1979) 2282.
[36] L. Nadjo, J.M. Savant, J. Electroanal. Chem. 48 (1973) 113.
[37] R.S. Nicholson, Anal. Chem. 37 (1965) 667.
[38] L.J. Nunez-Vergara, M.E. Ortiz, S. Bollo, J.A. Squella, Chem. Biol. Interactions 106 (1997) 1.
[39] J.A. Squella, S. Bollo, J. De Ia Fuente, L.J. Nunez-Vergara, Bioelectrochem. Bioeng. 34 (1994) 13.
[40] J. Carbajo, S. Bollo, L.J. Nunez-Vergara, P. Navarrete, J.A. Squella, J. Electroanal. Chem. 494 (2000) 69.
[41] M. Stankovich, A. Bard, J. Electroanal. Chem. 75 (1977) 487.